ELSEVIER

Journal of Molecular Catalysis A: Chemical 122 (1997) 147–157

JOURNAL OF MOLECULAR CATALYSIS A: CHEMICAL

Characterization and catalysis of a SiO_2-supported $[Au_6Pt]$ cluster $[(AuPPh_3)_6Pt(PPh_3)]^{2+}/SiO_2$

Youzhu Yuan [a,b], Kiyotaka Asakura [c], Huilin Wan [b], Khirui Tsai [b], Yasuhiro Iwasawa [a,*]

[a] *Department of Chemistry, Graduate School of Science, The University of Tokyo, Hongo, Bunkyo-ku, Tokyo 113, Japan*

[b] *Department of Chemistry and the State Key Laboratory of Physical Chemistry for Solid Surface, Xiamen University, Xiamen 361005, China*

[c] *Research Center for Spectrochemistry, Faculty of Science, The University of Tokyo, Hongo, Bunkyo-ku, Tokyo 113, Japan*

Received 18 September 1996; accepted 28 November 1996

Abstract

Structures and catalytic properties of a SiO_2-supported $[Au_6Pt]$ cluster, $[(AuPPh_3)_6Pt(PPh_3)](NO_3)_2$ (**1**), were characterized by FT-IR, in-situ EXAFS, and TPR, and also by the reactions such as H_2–D_2 equilibration, ethene hydrogenation, and CO oxidation to get insight into the key issues of metal catalysis. The cluster **1** was supported on SiO_2 without fragmentation of the cluster framework at room temperature under Ar atmosphere. The cluster framework of $\mathbf{1}/SiO_2$ was stable up to 400 K under vacuum. EXAFS analysis revealed that after heat-treatment of $\mathbf{1}/SiO_2$ at 473 K under vacuum the coordination numbers of Pt–Au and Au–Au(Pt) decreased compared to those for the original clusters due to cluster deformation and after treatment of $\mathbf{1}/SiO_2$ at 773 K the Au particles and Pt–$P^{\#}$ species ($P^{\#}$: phosphine species) were produced. The combination of TPR and EXAFS showed that the reduction at 603 K caused complete cleavage of Pt–Au and Au–$P^{\#}$ bonds accompanied with the formation of Au particles, while Pt–$P^{\#}$ bonds remained at 773 K. The incipient $\mathbf{1}/SiO_2$ showed catalytic activity in H_2–D_2 and ethene hydrogenation at 303 K without change of the cluster framework. The catalysis of $\mathbf{1}/SiO_2$ was suggested to be referred to the platinum atom which was embedded in the six gold cluster by the results of CO-adsorption, EXAFS, and pulse reaction analysis. This is contrasted to the fact that both $Pt(PPh_3)_4/SiO_2$ and $[Au_9(PPh_3)_8](NO_3)_3/SiO_2$ showed no catalytic activity for these reactions.

Keywords: Supported bimetallic $[Au_6Pt]$ cluster, H_2–D_2 equilibration; Characterization by FT-IR; In-situ EXAFS and TPR

1. Introduction

There has been currently significant interests in gold from both fundamental and industrial points of view, because Au is known as a good promoter for transition metal in catalysis and small Au particles on oxides such as α-Fe_2O_3, Co_3O_4 and TiO_2 also exhibit high catalytic activity for low-temperature oxidation of CO (for examples of Pt–Au catalysts, see Ref. [1], for examples of supported Au catalysts, see Ref. [2]). Evaporating gold on platinum single-crystal surface shows different activity and selectivity from those of the monometallic Pt catalyst for conversion of *n*-hexene [3,4]. It is believed that

* Corresponding author. Fax: +81-3-58006892; e-mail: iwasawa@utsc.s.u-tokyo.ac.jp.

PII S1381-1169(97)00004-6

alloys are formed between Group VIII metal such as Pt and IB element such as Au to alter the catalytic properties of platinum. Improved selectivity as well as suppressed deactivation are also beneficial aspects of these alloy catalysts. The 'alkali-metal-like' $d^{10}s^1$ electronic configuration of Au atom leads to relatively a tractable electronic structure compared to those for clusters of transition-metals with open d shells, which provides the theoretically interesting object particularly relevant to catalysis of the precious-metal–gold clusters. These studies can provide useful insight into reactivity of heteronuclear gold clusters and also provide a better understanding of metal–metal bonding and of synergistic effects in bimetallic catalysis. Recent advances in metal cluster syntheses may provide many opportunities to probe such modification at a molecular level in both homogeneous and heterogeneous systems [5–12]. Irrespective of large range of heterometallic cluster compounds containing gold synthesized to date, catalysis of only a few samples has been reported [13,14].

Recently, Pignolet et al. reported feasible application of cationic, phosphine-ligand stabilized AuPt clusters to heterogeneous catalysis by supporting them on SiO_2 and Al_2O_3 from surface organometallic interest [15–17]. They demonstrated that phosphine-ligated cationic clusters can be immobilized intactly on the oxide supports from the results of UV-VIS spectra and MAS ^{31}P NMR, and that the immobilization causes significant changes in catalytic activity. We independently reported characterization and performance of the catalyst obtained by supporting a bimetallic cluster $(AuPPh_3)_6Pt(PPh_3)](NO_3)_2$ (1) on SiO_2 [18]. The EXAFS data revealed that the cluster was stable enough to adsorb essentially intact on SiO_2 without destruction of the framework. The catalyst $\mathbf{1}/SiO_2$ is reported to have a catalytic activity (turnover frequency) of 29.8 s^{-1} for H_2–D_2 equilibration at 303 K. Here we will present the surface structure characterization and catalytic performance of $\mathbf{1}/SiO_2$ by means of EXAFS, FT-IR, and TPR and kinetic measurements to examine the properties generated by heterogenization Au_6Pt cluster with the structure of a Pt atom embedded in Au_6 ensemble.

2. Experimental

2.1. Materials and catalyst preparation

A dark-yellow microcrystalline $[(AuPPh_3)_6Pt(PPh_3)](NO_3)_2$ (**1**) was synthesized according to the literature [19]. The framework of **1** is shown in Fig. 1. Silica (Aerosil 300) was heated at 673 K for 1 h under vacuum before using as a support. The treated silica was impregnated with a carefully dried ethanol solution of **1**, followed by evacuation to remove the solvent. The loading of **1** was controlled to be 0.5 ~ 1.0 wt% based on Pt for the convenience of EXAFS measurements and CO and H_2 adsorption. All procedures were conducted in Ar atmosphere (99.9999%) to avoid contact with air.

2.2. Infrared spectroscopy

A pressed SiO_2 disk was placed in an IR cell with two NaCl windows, combined with a closed circulating system. The disk was heated at 673 K for 1 h in the cell, and impregnated dropwise with an ethanol solution of **1** in an Ar (99.9999%) atmosphere without contacting air. The supported cluster samples thus obtained were treated under vacuum at room temperature for 4 h. The FT-IR spectra were taken at 298 K

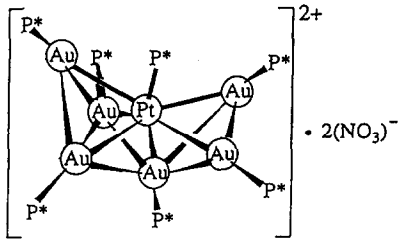

Fig. 1. Framework of the cluster **1**; P* = triphenylphosphine.

after treatment at different temperatures under vacuum on a JEOL JIR-7000 spectrometer. A SiO_2 background spectrum was subtracted from the observed ones of the samples.

2.3. Temperature-programmed reduction (TPR)

TPR spectra were recorded in a fixed-bed flow reaction system equipped with a gas chromatograph. A dry-ice/acetone trap was used to eliminate the influences of water and hydrocarbon. The samples were treated at room temperature for 2 h under flowing argon and then switched to a reduction gas of 5% H_2/Ar with a flow-rate of 30 ml/min, and heated up to 773 K at a heating rate of 10 K/min for TPR measurements.

2.4. Extended X-ray absorption fine structure (EXAFS) spectroscopy

Au L_3-edge and Pt L_3-edge EXAFS spectra were measured in a transmission mode at room temperature at BL-10B of the Photon Factory in the National Laboratory for High Energy Physics (KEK-PF) (proposal No.: 95G200). The measurements were carried out with a beam current of 250–350 mA and a storage-ring energy of 2.5 GeV in a transmission mode. The incident and transmitted x-rays were monitored by ionization chambers filled with N_2 and Ar(15%)–N_2(85%) gases, respectively. The samples were treated in a U-shape glass-tube connected to a closed circulating system, where the samples were treated at 400 K, or 473 K, or 773 K. The samples were also treated in the U-shape glass tube connected to a TPR measurement system, where the samples were reduced at given temperatures under a 5%H_2/Ar atmosphere. The treated samples were transferred to EXAFS cells, directly connected to the U-shape glass-tubes, without contacting air.

The analysis of EXAFS was performed by a curve-fitting method, using theoretically derived phase-shift and amplitude functions. The interactions of Pt–Au, Au–Au, Pt–P, Au–P, and Pt–Au–P were calculated by using the FEFF software [20]. Parameters used for FEFF calculations were listed in Table 1. The synthesized cluster **1**, Pt foil, Au foil, $Pt(PH_3)_4$ and $Au(PH_3)_4$ were used to determine the amplitude reduction factor S and to check the validity of these theoretically derived parameters. On the present analysis we took into account the error estimation recommended by international XAFS workshop on standards and criteria.

2.5. H_2–D_2 equilibration, ethene hydrogenation and CO oxidation

H_2/D_2 equilibration was tested in a fixed-bed flow reaction system equipped with a mass spectrometer. Ar was used as a diluent gas in a flow rate of 50 ml/min ($H_2 = D_2 = 2.0$ ml/min). The calibrations for mass spectrometer signals of H_2, D_2 and HD were conducted

Table 1
Structural data and Fourier transform ranges used for FEFF calculations

Parameters used for FEFF calculations			Fourier transform range	
Shell	N	r (Å)	Δk (Å^{-1})	Δr (Å)
Pt–P for $Pt(PPh_3)$	1.0	2.28	3.0 ~ 9.0	1.42 ~ 2.30
Pt–Au for Pt(Au)	1.0	2.68	3.0 ~ 9.0	2.40 ~ 3.20
Pt–Pt for Pt foil	1.0	2.78	3.0 ~ 9.0	2.10 ~ 3.15
Au–P for $Au(PPh_3)$	1.0	2.30	3.0 ~ 12.0	1.42 ~ 2.30
Au–Au for Au(Au) or Au(Pt)	1.0	2.87	3.0 ~ 12.0	2.40 ~ 3.20
Au–Au for Au foil	1.0	2.87	3.0 ~ 16.0	2.10 ~ 3.15

N: coordination number for absorber–backscatterer pair; r: interatomic distance; Δk: range used for Fourier transformation (k is the wave vector); Δr: range used for inverse Fourier transformation (r is the distance).

under the same condition as in the reaction. Pulse experiments were carried out in the same system by using Ar as a carrier gas in a flow rate of 100 ml/min. At this flow rate the mean residence time in the reactor was less than 2 s. Purchased Ar, D_2, H_2, CO, and ethene of 99.999% purity were used without further purification.

Ethene Hydrogenation and CO oxidation were carried out under the condition of C_2H_4:H_2 = 13:13 kPa and CO:O_2 = 13:13 kPa in a closed circulating system. The products in ethene hydrogenation and CO oxidation were analyzed by a gas chromatograph using VZ-10 and Unibeads C columns, respectively.

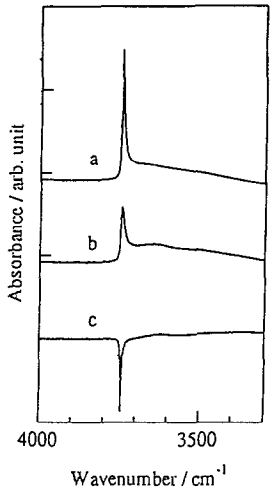

Fig. 3. Changes in the intensity of the ν(OH) peak by supporting the cluster **1** on SiO_2 at room temperatures; (a) SiO_2 pretreated at 673 K, (b) after supporting **1** on SiO_2 followed by evacuation, (c) the difference spectrum (a)–(b).

3. Results

3.1. Chemisorption of cluster 1 on SiO_2

When an ethanol solution of cluster **1** was brought into contact with a silica gel pretreated at 673 K under a high purity of Ar, the initial deep yellowish color became pale within several minutes. After the evacuation the supported cluster **1** was characterized by skeleton vibration of aryl group and the characteristic band of nitrate group by FT-IR. Fig. 2(a), (b), (c) are the spectra for PPh_3 on SiO_2, cluster **1** on SiO_2, and cluster **1** mixed with KBr, respectively. The bands attributed to PPh_3 ligands are almost the same among these samples, consistent with the hypothesis that the cluster framework did not decompose on the SiO_2 surface. However, the spectrum for $\mathbf{1}/SiO_2$ did not show υ_{NO} peak at 1385 cm^{-1} characterizing the nitrate ionic counterpart of cluster **1**. The spectra in the υ_{OH} region for OH groups of SiO_2 before and after supporting **1** are shown in Fig. 3(a), (b), respectively. The intensity of the υ_{OH} peak at ca. 3740 cm^{-1} decreased by supporting **1** as proved in the difference spectrum shown in Fig. 3(c). These results indicate that the OH groups on SiO_2 surface reacted with the NO_3^- anions in the cluster probably through the ionic exchange reaction to form HNO_3 which can be eliminated during the evaporation of the sample.

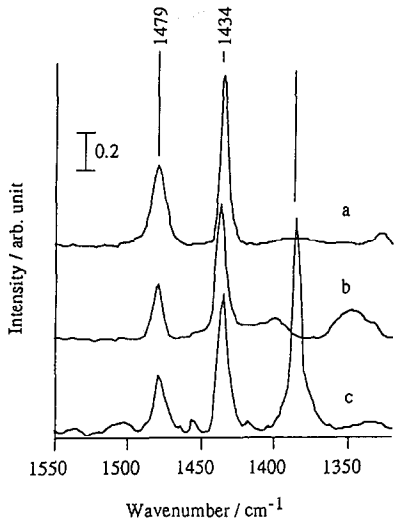

Fig. 2. FT-IR of PPh_3/SiO_2, $\mathbf{1}/SiO_2$, and **1** mixed with KBr. (a) PPh_3/SiO_2, (b) $\mathbf{1}/SiO_2$, (c) **1** + KBr.

3.2. TPR performance of 1 / SiO_2

TPR spectra of the incipient $\mathbf{1}/SiO_2$ and the $\mathbf{1}/SiO_2$ treated at 473 K under vacuum are shown in Fig. 4(a), (b). Reduction of the intact $\mathbf{1}/SiO_2$ started at about 373 K and the TPR

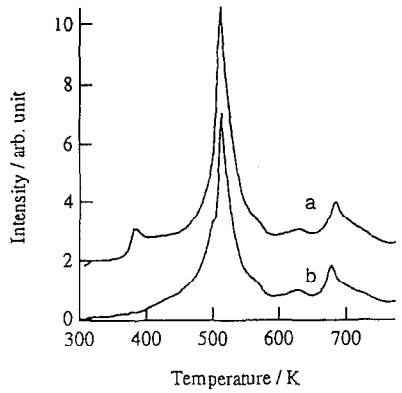

Fig. 4. TPR spectra of $1/SiO_2$; (a) the incipient $1/SiO_2$; (b) $1/SiO_2$ treated 473 K.

spectrum showed three peaks around 380, 520 and 680 K.. In the TPR of the $1/SiO_2$ treated at 473 K, the first peak was not observed, but other two peaks remained essentially unchanged. The results imply that the cluster structure of the supported $[Au_6Pt]$ species a little changed by the heat-treatment at 473 K, but still remains without destruction.

3.3. EXAFS observations during heat-treatment

EXAFS spectra of $1/SiO_2$ treated at 400, 473, and 773 K are shown in Fig. 5. Fig. 5(A) shows the EXAFS oscillation of Au L_3-edge for the incipient $1/SiO_2$ and its Fourier transform with three peaks around 2.0, 2.4 and 2.8 Å (phase shift uncorrected), which are assignable to Au–P, Au–Pt and Au–Au bonds, respectively. Fig. 5(B) shows the EXAFS oscillation and its Fourier transform for the $1/SiO_2$ treated at 400 K, which are similar to those for $1/SiO_2$ (Fig. 5(A)). After treatment of $1/SiO_2$ at 473 K under vacuum, a decrease in intensity of the EXAFS Fourier transform for the peak around 2.7 Å was observed in Fig. 5(C). When $1/SiO_2$ was treated at 773 K under vacuum, the EXAFS data dramatically changed as shown in Fig. 5(D) which is due to the contribution of Au particles. The distance and the coordination number of the Au–Au bond were determined to be 2.87 Å and 10.0, respectively, by curve-fitting analysis (Fig. 6). The best fitting results are listed in Table 2. It is suggested that the cluster framework was decomposed to form metallic gold particles on SiO_2 surface at 773 K under vacuum.

Fig. 7(A) shows the EXAFS oscillation of Pt L_3-edge for the incipient $1/SiO_2$ and its Fourier transform with two peaks around 2.0 and 2.6 Å (phase shift uncorrected), which are assigned to Pt–P and Pt–Au bonds. The EXAFS oscillation

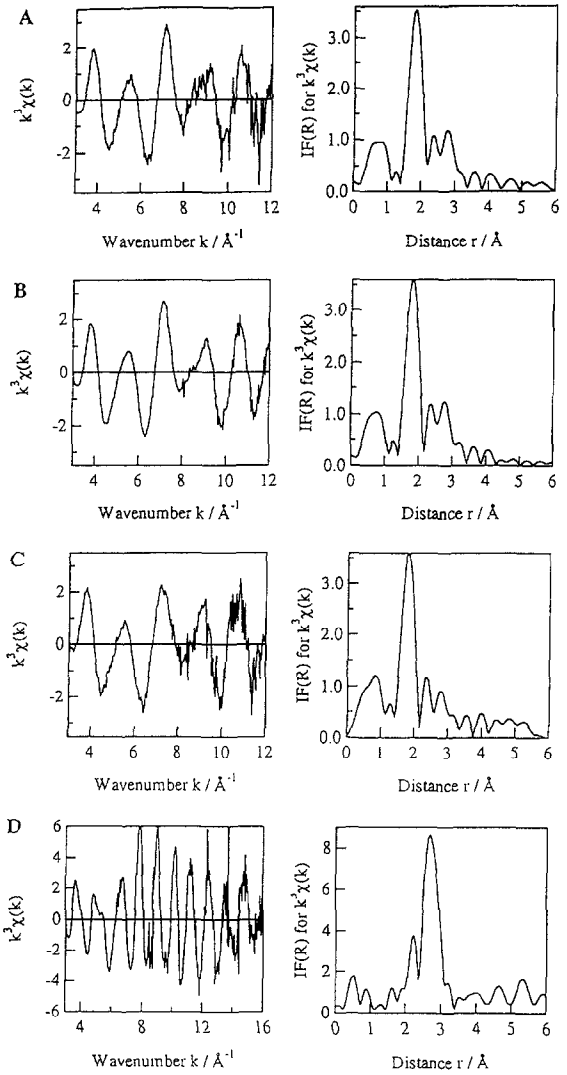

Fig. 5. EXAFS oscillations and Fourier transforms for the Au L_3-edge data; (A) the incipient $1/SiO_2$, (B) $1/SiO_2$ treated at 400 K, (C) $1/SiO_2$ treated at 473 K, (D) $1/SiO_2$ treated at 773 K.

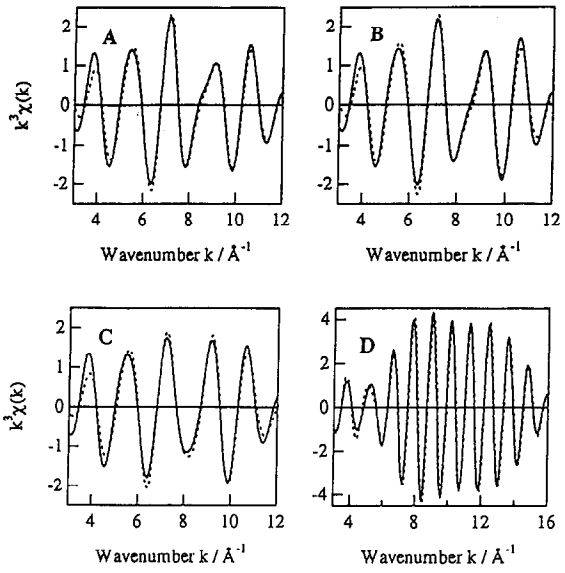

Fig. 6. The curve-fitting analysis based on the two-shell model of Au–P and Au–Au(Pt) for $1/SiO_2$: ————, observed, ..., calculated. (A) the incipient $1/SiO_2$, (B) $1/SiO_2$ treated at 400 K, (C) $1/SiO_2$ treated at 473 K, (D) $1/SiO_2$ treated at 773 K.

of Pt L_3-edge and its associated Fourier transform for the $1/SiO_2$ treated at 400 K under vacuum (Fig. 7B)) were almost the same as those of the incipient $1/SiO_2$. By heating the 1/SiO2 at 473 K the intensity of the peak around 2.6 decreased a little(Fig. 7(C)). No Pt–Au(Pt) bond was observed for the $1/SiO_2$ treated at 773 K under vacuum as shown in Fig. 7(D), where only a peak around 2.0 was observed. The curve-fitting results for the EXAFS data are shown in Fig. 8 and the obtained bond distance and coordination number are listed in Table 3.

3.4. EXAFS observations during TPR

EXAFS spectra of $1/SiO_2$ during TPR were observed for the samples heated to 423 K, 603 K, and 773 K under the TPR condition. Fig. 9 shows the Fourier transforms of the EXAFS data at Au L_3-edge and Pt L_3-edge for $1/SiO_2$ reduced at 423 K, 603 K and 773 K. By comparison with the EXAFS Fourier transforms for the incipient $1/SiO_2$ in Fig. 5(A) and Fig. 7(A), the peaks in Fig. 9(A) are straightforwardly assigned to the bonds of Au–P and Au–Pt(Au), and Pt–P and Pt–Au, respectively for the Au L_3-edge Fourier transform and the Pt L_3-edge Fourier transform. The best-fit results are listed in Table 4. The data demonstrate no change in the cluster framework of $1/SiO_2$ by TPR up to 423 K within the limitation of EXAFS analysis. After raising the temperature to 603 K, however, the Au L_3-edge EXAFS Fourier transform exhibited only one peak which was assigned to

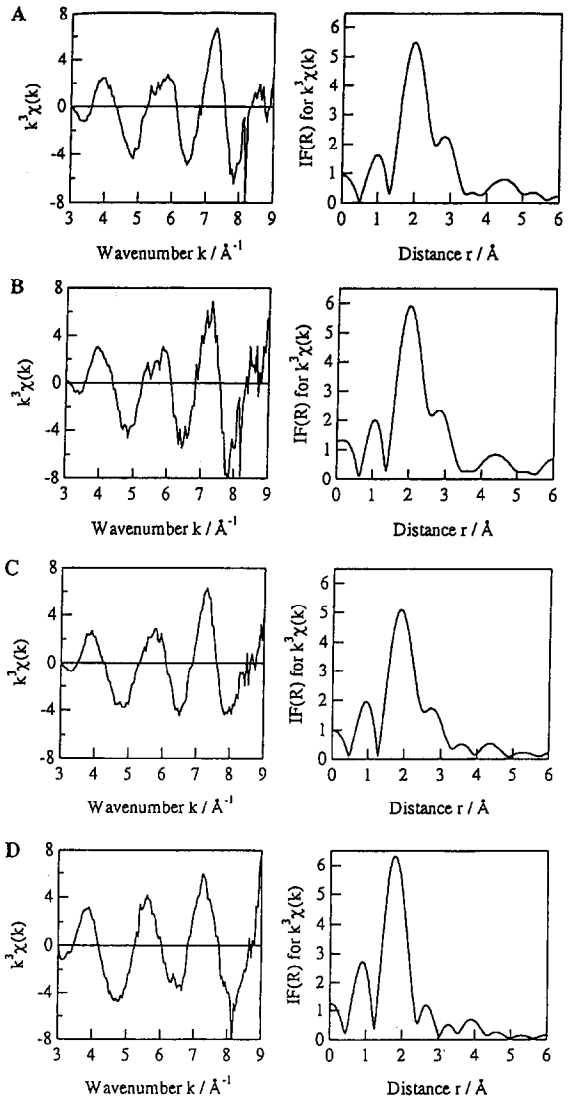

Fig. 7. EXAFS oscillations and Fourier transforms for the Pt L_3-edge data; (A) the incipient $1/SiO_2$, (B) $1/SiO_2$ treated at 400 K, (C) $1/SiO_2$ treated at 473 K, (D) $1/SiO_2$ treated at 773 K.

Table 2
Curve-fitting results for Au L_3-edge EXAFS data of $\mathbf{1}/SiO_2$ under vacuum

	Au–P				Au–Au(Pt)				R_f (%)
	N	r (Å)	$\Delta\sigma^2$ (Å^2)	ΔE (eV)	N	r (Å)	$\Delta\sigma^2$ (Å^2)	ΔE (eV)	
$\mathbf{1}/SiO_2$	1.0 ± 0.1	2.30 ± 0.01	0.0 ± 0.001	4 ± 4	4.0 ± 0.2	2.83 ± 0.02	0.0 ± 0.001	2 ± 4	1.8
$\mathbf{1}/SiO_2$ [a]	1.0 ± 0.1	2.30 ± 0.01	0.0 ± 0.001	3 ± 4	4.0 ± 0.2	2.83 ± 0.02	0.002 ± 0.001	4 ± 4	2.2
$\mathbf{1}/SiO_2$ [b]	0.6 ± 0.1	2.28 ± 0.02	0.0017 ± 0.0009	4 ± 4	3.0 ± 0.3	2.83 ± 0.02	0.004 ± 0.001	2 ± 3	3.1
$\mathbf{1}/SiO_2$ [c]					10.0 ± 1.0	2.87 ± 0.02	0.004 ± 0.001	0.6 ± 4	1.0
$\mathbf{1}$ [d]	(1.0)	(2.30)			(4.0)	(2.83)			

N: coordination number, r: interatomic distance, σ: Debye–Waller factor, ΔE: difference in the origin of photoelectron energy between reference and sample, R_f: residual factor in the curve fitting.
[a] Treated at 400 K.
[b] Treated at 473 K.
[c] Treated at 773 K.
[d] Crystallographic data of cluster **1**. Au–Au (Au foil): 2.87 Å.

Table 3
Curve-fitting results for Pt L_3-edge EXAFS data of $\mathbf{1}/SiO_2$ under vacuum

Sample	Pt–P				Pt–Au				R_f(%)
	N	r (Å)	$\Delta\sigma^2$ (Å^2)	ΔE (eV)	N	r (Å)	$\Delta\sigma^2$ (Å^2)	ΔE (eV)	
$\mathbf{1}/SiO_2$	1 ± 0.2	2.28 ± 0.02	0.0 ± 0.001	6 ± 4	6 ± 0.2	2.69 ± 0.02	0.0 ± 0.001	0.3 ± 4	1.1
$\mathbf{1}/SiO_2$ [a]	1 ± 0.2	2.28 ± 0.02	0 ± 0.001	8 ± 4	6 ± 0.2	2.69 ± 0.02	0.001 ± 0.001	0.1 ± 5	1.1
$\mathbf{1}/SiO_2$ [b]	1.3 ± 0.3	2.27 ± 0.02	0.001 ± 0.001	5 ± 5	4.1 ± 0.2	2.69 ± 0.02	0.003 ± 0.001	3 ± 4	1.2
$\mathbf{1}/SiO_2$ [c]	3.3 ± 0.6	2.28 ± 0.02	0.002 ± 0.001	2 ± 5					1.3
$\mathbf{1}$ [d]	(1.0)	(2.28)			(4.0)	(6.0)	(2.69)		

[a] Treated at 400 K.
[b] Treated at 473 K.
[c] Treated at 773 K.
[d] Cluster **1**.

Table 4
Curve-fitting results for Au L_3-edge EXAFS data of $\mathbf{1}/SiO_2$ during TPR

T (K)	Au–P				Au–Au(Pt)				R_f (%)
	N	r (Å)	$\Delta\sigma^2$ (Å^2)	ΔE (eV)	N	r (Å)	$\Delta\sigma^2$ (Å^2)	ΔE (eV)	
423	1 ± 0.1	2.28 ± 0.02	0.001 ± 0.001	4 ± 4	3.6 ± 0.8	2.8 ± 0.02	0.000 ± 0.001	3 ± 4	1.6
603					11.1 ± 1.0	2.87 ± 0.02	0.001 ± 0.001	1 ± 4	2.7
773					11.2 ± 1.0	2.87 ± 0.02	0.001 ± 0.001	1 ± 4	1.6

Table 5
Curve-fitting results for Pt L_3-edge EXAFS data of $\mathbf{1}/SiO_2$ during TPR

T (K)	Pt–P				Pt–Au				R_f (%)
	N	r (Å)	$\Delta\sigma^2$ (Å^2)	ΔE (eV)	N	r (Å)	$\Delta\sigma^2$ (Å^2)	ΔE (eV)	
423	1 ± 0.1	2.3 ± 0.02	0.001 ± 0.001	4 ± 4	4.9 ± 0.8	2.8 ± 0.02	0.001 ± 0.001	3 ± 4	0.1
603	2.8 ± 0.6	2.28 ± 0.02	0.001 ± 0.001	0.4 ± 4					2.6
773	3.2 ± 0.7	2.27 ± 0.02	0.003 ± 0.001	0.7 ± 4					2.7

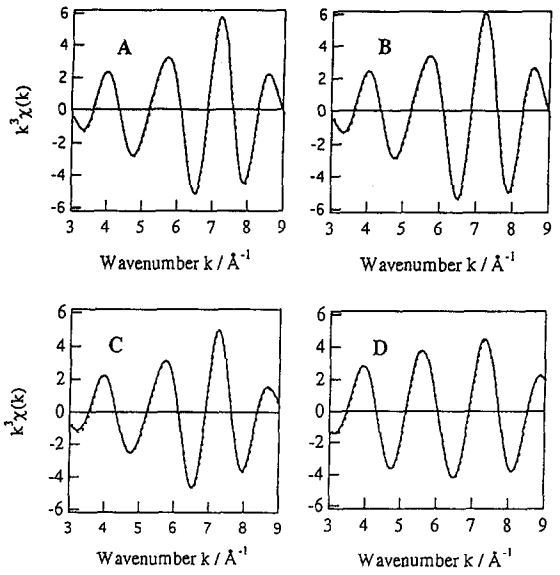

Fig. 8. The curve-fitting analysis based on the two-shell model of Pt–P and Pt–Au for $1/SiO_2$: ————, observed, ..., calculated. (A) the incipient $1/SiO_2$, (B) $1/SiO_2$ treated at 400 K, (C) $1/SiO_2$ treated at 473 K, (D) $1/SiO_2$ treated at 773 K.

Au–Au bond. The curve fitting analysis for this peak revealed a bond distance of 2.87 Å and a coordination number of 11.1 as shown in Table 4, indicating the formation of metallic Au particles on SiO_2 surface at 603 K. After heating the sample of Au–Au bond to 773 K, the Au particles still have the distance and coordination number of Au–Au bond similar to those for the sample at 603 K. On the other hand the Fourier transforms for the Pt L_3 edge-EXAFS showed that the Pt–P$^{\#}$ contribution (P$^{\#}$: phosphine species) increased gradually throughout the TPR measurement. The coordination number of Pt–P$^{\#}$ increased from 1.0 at 423 K to 2.8 at 603 K or to 2.5 at 773 K in the TPR (Table 5).

Table 6
H_2–D_2 equilibration (a), ethene hydrogenation (b) and CO oxidation (c) over several catalysts at 303 K

Catalysts	TOF/s^{-1}		
	(a)	(b)	(c)
1	2.0		
$1/SiO_2$	29.8	8×10^{-4}	7×10^{-5}
$1/SiO_2$ treated at 473 K	11.1	5×10^{-4}	3×10^{-5}
$Pt(PPh_3)_4/SiO_2$	0.0	0.0	0.0
$Pt(PPh_3)_4/SiO_2$ treated at 473 K	0.0	0.0	0.0
$[Au_9(PPh_3)_8](NO_3)_3/SiO_2$	0.0	0.0	0.0

3.5. Catalysis of 1 / SiO_2

H_2–D_2 equilibration on $1/SiO_2$ at 303 K was carried out in a fixed-bed flow reactor. The catalytic reaction rates (turnover frequency; TOF) are shown in Table 6, where TOF is defined as (mol of HD)(mol of cluster)$^{-1}$ (s)$^{-1}$. The activity of **1** in the solid state was promoted about 15 times by supporting **1** on SiO_2. Pignolet and coworkers also observed similar enhancement of the reaction rate by supporting [16,17]. The increase in activity may be attributed mainly to a high surface area of the support. It is to be noted that the catalytic activity of the incipient $1/SiO_2$ was higher than that of the sample treated at 473 K. $[Au_9(PPh_3)_8](NO_3)_3/SiO_2$ was inactive for H_2–D_2 equilibration and $Pt(PPh_3)_4/SiO_2$ was also inactive as shown in Table 6.

The results of catalytic ethene hydrogenation and CO oxidation in a closed circulating system are also shown in Table 6. It was found that the hydrogenation of ethene to ethane over $1/SiO_2$ proceeded at an initial rate of 8×10^{-4} s^{-1} at 303 K. The incipient $1/SiO_2$ also catalyzed a very low reaction rate of CO oxidation (TOF of 7×10^{-5} s^{-1}). TPR spectra and EXAFS data for $1/SiO_2$ before and after ethene hydrogenation were the same, suggesting that no change occurred in the cluster framework of $1/SiO_2$ during the ethene hydrogenation.

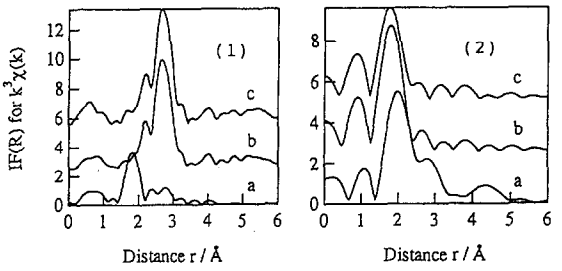

Fig. 9. Fourier transforms of the EXAFS oscillation at Au L_3-edge (1) and Pt L_3-edge (2) for $1/SiO_2$ during TPR; (a) $1/SiO_2$ reduced by TPR to 423 K, (b) $1/SiO_2$ reduced by TPR to 603 K, (c) $1/SiO_2$ reduced by TPR to 773 K.

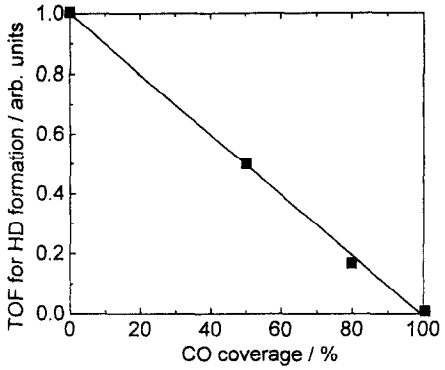

Fig. 10. CO inhibition: linear decrease of the TOF for H_2–D_2 equilibration by CO coverage.

3.6. Pulse reaction

In order to obtain information on active sites, the 1 ml pulse of a mixture of H_2, D_2, and C_2H_4(1:1:1) was admitted to a 100 ml/min Ar flow and the products were monitored by mass spectroscopy. About 80% decrease in the rate of H_2–D_2 equilibration by the presence of C_2H_4 was observed. No ethane was formed, while a very small amount of C_2H_3D was detected. When a mixture of C_2H_4 and D_2 was added as a pulse to the Ar flow, the HD formation was 1/20 as large as that in a H_2–D_2 pulse reaction and the amount of C_2H_3D formed was the similar amount to that in the pulse reaction of H_2–D_2–C_2H_4. No H_2–D_2 equilibration proceeded when CO was pulsed to a gas flow of H_2–D_2.

3.7. CO poisoning effect on H_2–D_2 equilibration

The addition of molar excess of CO pulse to an Ar flow through $1/SiO_2$, followed by Ar purge, resulted in the complete poisoning of H_2–D_2 equilibration. By Ar flowing CO gradually desorbed accompanying by partial recovery of H_2–D_2 equilibration. The catalytic activity was completely recovered after CO desorption. We monitored the amount of desorbed CO by an on-line GC and calculated the remained CO coverage on the cluster. The TOF for H_2–D_2 equilibration was plotted against CO coverage in Fig. 10.

4. Discussion

4.1. Adsorption of 1 on SiO_2 and structure behavior of 1 / SiO_2

The FT-IR spectra in Fig. 2 and the color of the solid which is sensitive to the coordination sphere in the cluster demonstrate that the cluster **1** is supported on SiO_2 with retention of the original cluster framework structure. The comparison of the IR spectrum of the cluster in KBr with that of the supported cluster, along with the decrease of the surface OH peak intensity by supporting the cluster **1** on SiO_2 suggests that the cluster–surface interaction occurred with the nitrate anions which reacted with the surface OH groups to form the surface bimetallic cluster, probably evolving HNO_3, as shown in Fig. 11. Thus it is proposed that the cluster was supported on SiO_2 by an ion exchange reaction, without loss of the strong interactions between Au and Pt metals.

The retention of the cluster framework was also characterized by EXAFS, The data in Ta-

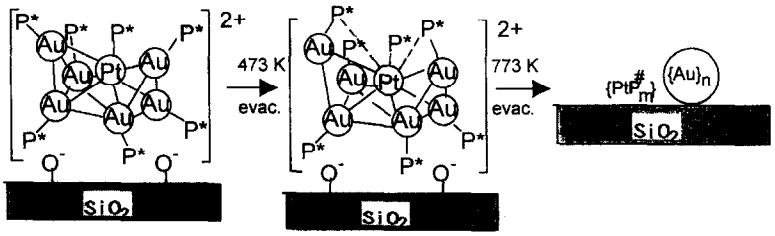

Fig. 11. Cluster framework transformation in $1/SiO_2$ by heating in vacuum. Dotted lines are tentatively represented. $P^{\#}$ = phosphine species.

bles 2 and 3 demonstrate the cluster framework in $1/SiO_2$ retains its original structure after deposition on the SiO_2 surface, keeping the Pt–Au and Au–Au distances unchanged. The cluster framework is stable up to 400 K under vacuum. However, part of metal–metal bonds of **1** on SiO_2 at 470 K under vacuum is cleaved, judging from the results of the bond numbers of Au–Au(Pt) and Pt–Au which decreased to about 75% (Table 2) and 68% (Table 3) of the original ones, respectively, and also from a small increase in the coordination number of Pt–$P^{\#}$ ($P^{\#}$: phosphine species). The TPR spectrum of the sample treated at 473 K was essentially the same as that of the incipient cluster in the temperature range above 400 K. It is likely that a local rearrangement of the cluster framework occurred at 473 K as proposed in Fig. 11. When the $1/SiO_2$ was heated at 773 K, the cluster of $1/SiO_2$ was completely destroyed to form metallic gold particles (Table 2) and Pt–$(P^{\#})_n$ ($n = 3$, Table 3) species when heated to 773 K (Fig. 11). No Pt–Au bonding was detected with the sample treated at 773 K.

The curve-fitting results of the EXAFS data during TPR of $1/SiO_2$ demonstrate the complete cleavage of Au–Pt and Au–P bonds to form Au particles at 603 K (Table 4 and Fig. 9). The TPR spectrum of Fig. 4 showed a principle peak around 420 K, which may be related to the destruction of the cluster framework characterized by EXAFS. The remaining Phosphine species coordinate to Pt atom even if the TPR temperature was reached to 773 K [1]. The formation of Au particles on SiO_2 surface by heat-treatment of $1/SiO_2$ under vacuum or in a flow of 5% H_2/Ar atmosphere indicates that the Au–P bond and the Au–Pt bond were much weaker than the Pt–P bond. Thus Pt–Au bimetallic particles may not be prepared by using a phosphine-stabilized Pt–Au cluster as precursor. However, the results also may imply that phosphine-stabilized gold clusters as precursors provide a method for preparation of supported ultra fine gold particles on appropriate oxides.

4.2. Catalytic site and synergism in $1/SiO_2$

It was found that the adsorption of an equimolar CO on the $[Au_6Pt]$ cluster supported on SiO_2 completely suppressed the H_2–D_2 equilibration as shown in Fig. 10. The CO poisoning was proportional to the CO coverage(coverage: amount of adsorbed CO/Pt atoms). By exposing $1/SiO_2$ to CO, yellowish color of $1/SiO_2$ immediately turned to orange-red; the CO-adsorbed $1/SiO_2$ may resemble the CO adduct of **1** in solution [15,16]. The CO adsorption on Pt atom in $1/SiO_2$ is also characterized by EXAFS which revealed the distortion of the metal phosphine bond angle [21]. Thus it is concluded that the Pt atom in the cluster **1** supported on SiO_2 contributes to the H_2–D_2 equilibration as active site. This is contrasted to the catalysis of Pt particles in which multi-site of Pt atoms are believed to be demanded for activation of hydrogen and H_2–D_2 equilibration.

Lower activity of $1/SiO_2$ treated at 473 K compared to $1/SiO_2$ is possibly referred to the increase in the coordination number of Pt–P bonds and to the decrease in the coordination number of Au–Pt bonds. The monometallic catalysts of $Pt(PPh_3)_4/SiO_2$ and that pretreated at 473 K were inactive, which suggests that Au–Pt bonds may participate or play a synergistic role in the activation of H_2.

5. Conclusions

The obtained results show that the cluster framework of **1** can be supported intactly on SiO_2 surface. The NO_3^- ionic counterpart in **1** is suggested to interact with the OH groups of

[1] By comparison, we conducted the EXAFS measurements for $Pt(PPh_3)_4/SiO_2$ after TPR at 773 K under the condition for $1/SiO_2$. The results showed that the $P^{\#}$ species would bond to Pt atom and the coordination number is 2.8. The data is available upon request.

SiO_2 to form $[Au_6(PPh_3)_6Pt(PPh_3)OSi\lesssim]$. The cluster framework in $\mathbf{1}/SiO_2$ is stable up to 400 K without breaking of Au–Pt, Au–Au, Au–P* and Pt–P* bonds under vacuum. Local rearrangement in the cluster framework structure occurred when $\mathbf{1}/SiO_2$ was heated at 473 K. By heating to 773 K Au particles and Pt(P#) species are produced on SiO_2 surface. The destruction of the cluster framework may begin from a cleavage of Pt–Au bond, accompanied with migration of P* ligand from Au atom to Pt atoms.

The intact $\mathbf{1}/SiO_2$ shows a catalytic activity(TOF of 29.8 s^{-1}) for H_2–D_2 equilibration. The $\mathbf{1}/SiO_2$ also catalyzes ethene hydrogenation and CO oxidation at 303 K with much lower activity. The catalysis of $\mathbf{1}/SiO_2$ is due not to a platinum impurity but to the platinum atom which is embedded in the gold cluster framework. The catalytic reaction mechanism for H_2–D_2 equilibration on $\mathbf{1}/SiO_2$ may be different from that on Pt metallic particles.

References

[1] J.R.H. van Schaik, R.P. Dessing, V. Ponec, J. Catal. 38 (1975) 273; J.K.A. Clarke, L. Manninger, T. Baird, J. Catal. 54 (1978) 230; 9 (1984) 85; J.H. Sinfelt, Bimetallic Catalysts (Wiley, New York, 1985); R.C. Yates, G.A. Somorjai, J. Catal. 103 (1987) 208; K. Bakakrishnan, A. Sachdev, J. Sachwank, J. Catal. 121 (1990) 441; P.A. Sermon, J.M. Thomas, K. Keryou, G.R. Millward, Angew. Chem. Int. Ed. Engl. 26 (1987) 918; A. Sachdev, J. Schwank, J. Catal. 120 (1989) 353; K. Balakrishnan, J. Sachwank, J. Catal. 132 (1991) 451; D. Rouabah, J. Fraissard, J. Catal. 144 (1993) 30; J. Sachtler, K. Balakrishnan, A. Sachdev, in: L. Guczi, F. Solymosi and P. Tetenyi (Eds.), New Frontiers in Catalysis (Elsevier, Amsterdam, 1993) p. 905.

[2] N.W. Cant and W.K. Hall, J. Phys. Chem. 75 (1971) 2914; S. Galvagno and G. Parravano, J. Catal. 55 (1978) 178; J. Schwank, Gold Bull. 16 (1983) 103; M. Haruta, S. Tsubota, N. Yamada, T. Kobayashi and S. Iijima, J. Catal. 115 (1989) 301; M. Haruta, S. Tsubota, T. Kobayashi, H. Kageyama, M.J. Genet and B. Delmon, J. Catal. 144 (1993) 174; S. Tsubota, A. Ueda, H. Sakurai, T. Kabayashi and M. Haruta, ACS Symp. Ser. 552 (1993) 420.

[3] J. Sachtler and G. Somorjai, J. Catal. 81 (1983) 77.

[4] J. Sachtler, J. Biberian and G. Somorjai, Surf. Sci. 110 (1981) 43.

[5] P. Braunstein and J. Rose, in: I. Bernal (Ed.), Stereochemistry of Oganometallic and Inorganic Compounds, Vol. 3 (Elsevier, Amsterdam, 1988) ch. 1, p. 1.

[6] P. Braunstein and J. Rose, Gold Bull. 18 (1985) 17.

[7] G. Suss-fink, G. Meister, Adv. Organomet. Chem. 35 (1993) 41.

[8] B.C. Gates, L. Guczi, H. Knozinger (Eds.), Stud. Surf. Sci. Catal. 29 (1986).

[9] M. Ichikawa, Adv. Catal. 38 (1992) 283.

[10] Y. Iwasawa (Ed.), Tailored Metal Catalysis (Reidel, The Netherlands, 1986).

[11] Y. Iwasawa, Catal. Today 18 (1993) 21.

[12] B.C. Gates, Chem. Rev. 95 (1995) 511.

[13] K.P. Hall and D.M.P. Mingoss, Prog. Inorg. Chem. 32 (1981) 237.

[14] E. John and J. Gao, J. Chem. Soc. Chem. Commun. (1985) 39.

[15] I. Gubkina, L. Rubinstein and L. Pignolet, Abstr. ACS Meeting 208 (1994) 405.

[16] I. Graf, J. Bacon, M. Consugar, M. Curley, L. Ito and L. Pignolet, Inorg. Chem. 35 (1996) 689.

[17] M.A. Aubart, B.D. Chandler, R.A.T. Gould, D.A. Krogstad, M.J. Schoondergang and L.H. Pignolet, Inorg. Chem. 33 (1994) 3724.

[18] Y. Yuan, K. Asakura, H. Wan, K. Tsai and Y. Iwasawa, Chem. Lett. (1996) 129.

[19] L.N. Ito, J.D. Sweet, A.M. Mueting, L.H. Pignolet, M.F.J. Schoondergang and J.J. Steggerda, Inorg. Chem. 28 (1989) 3696.

[20] J.J. Rehr de Leon. J. Mustre, S.I. Zabinsky, R.C. Albers, J. Am. Chem. Soc. 113 (1991) 5235.

[21] K. Asakura, Y. Yuan and Y. Iwasawa, Proc. of XAFS-IX, Grenoble 1996, in press.